A Bluetooth Low Energy (BLE)-enabled Microdevice for Activity-dependent Stimulation in Nonhuman Primates

Nicholas H. Vitale[1], Christopher A. Delianides[1], David J. Guggenmos[2], Meysam Azin[1], Heather Hudson[2], Randolph J. Nudo[2], and Pedram Mohseni[1]

[1]Dept. of Electrical, Computer, and Systems Engineering, Case Western Reserve University, Cleveland, OH, USA
[2]Dept. of Rehabilitation Medicine, University of Kansas Medical Center, Kansas City, KS, USA
{pedram.mohseni@case.edu}

2021 IEEE Biomedical Circuits and Systems Conference (BioCAS) | 978-1-7281-7204-0/21/$31.00 ©2021 IEEE | DOI: 10.1109/BIOCAS49922.2021.9644956

***Abstract*—This paper reports on the design, fabrication, and assembly of a Bluetooth low energy (BLE)-enabled microdevice for activity-dependent stimulation (ADS) in nonhuman primates (NHPs). The microdevice is partitioned into two miniaturized head-mounted and backpack units with compact enclosures. The head-mounted unit houses a previously developed application-specific integrated circuit (ASIC) for ADS along with all the requisite peripheral hardware. The backpack unit houses power-management electronics and a BLE module for bidirectional wireless communication between the head-mounted unit and a BLE-enabled user base station. The overall microdevice weighs ~48g and consumes ~618μW from a lithium-ion battery (3.6V, 1.6Ah) placed in the backpack unit. Moreover, the overall functionality of the microdevice is experimentally demonstrated *in vitro* in saline via recording and discriminating neural spike waveforms as well as performing spike-triggered stimulation. The microdevice is envisioned for use in longitudinal experiments assessing the effects of ADS on facilitating functional recovery in an NHP model of traumatic brain injury.**

***Index Terms*–Activity-dependent stimulation, Bluetooth low energy, brain-machine interface, intracortical microstimulation, neural microdevice.**

I. Introduction

The adult brain is highly plastic, forming and re-forming new functional connections between different regions throughout the lifetime of an individual. Brain injury, as occurs in traumatic brain injury (TBI), is a potent trigger to initiate an extensive growth response within the brain, especially in areas anatomically connected to the injured region. Such self-repair mechanisms might be exploited to improve functional recovery after such injuries. Recent advances in our knowledge of network interactions within the normal and injured nervous system, especially the role played by so-called spike-timing-dependent plasticity to form communication links, have been a powerful impetus to develop device-based approaches for brain and spinal cord repair [1], [2].

We have previously developed a wireless microdevice for activity-dependent stimulation (ADS) to test such brain repair strategies in laboratory animals [3], and have demonstrated the remarkable ability of such an approach to improve functional connectivity in targeted brain pathways and induce rapid recovery of sensory-motor skills in a rodent model of TBI [1].

This work was supported by the Office of the Assistant Secretary of Defense for Health Affairs through the Joint Warfighter Medical Research Program under Award No. W81XWH-16-1-0503. Opinions, interpretations, conclusions and recommendations are those of the authors and are not necessarily endorsed by the Department of Defense.

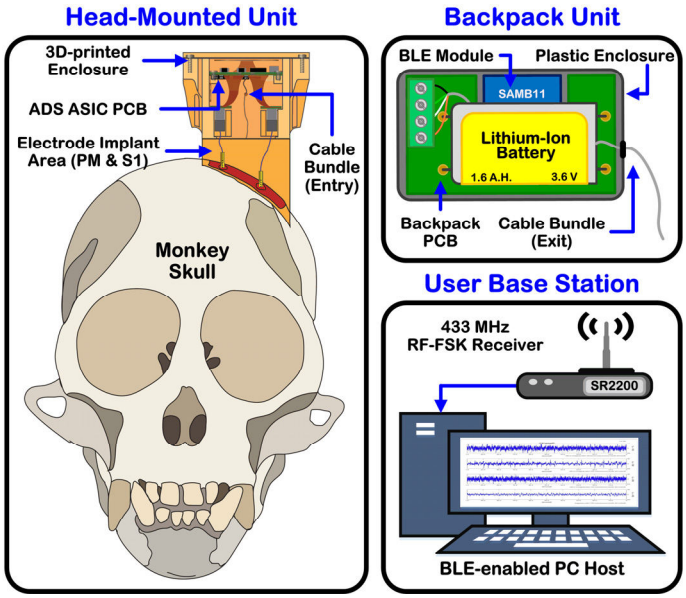

Fig. 1. Illustration of a skull-affixed head-mounted unit that can bidirectionally communicate with a user base station via a BLE-enabled backpack unit.

To further advance this technology toward implementation in human clinical populations, the efficacy of the ADS approach should be established in a more complex animal model such as a nonhuman primate (NHP).

In this paper, we report on the design, fabrication, assembly, and *in vitro* testing of a miniaturized microdevice for longitudinal experiments in an NHP (specifically, a squirrel monkey). Figure 1 shows an illustration of the microdevice comprising 1) a head-mounted unit packaged within a custom skull-affixed, 3D-printed, resin chamber and 2) a backpack unit worn inside a primate jacket. The backpack unit incorporates a Bluetooth low energy (BLE) module to establish a bidirectional, wireless, communication link between the head-mounted unit and a BLE-enabled PC host functioning as the user base station. The head-mounted unit is also interfaced with a pair of penetrating microelectrode arrays for recording neural activity from the premotor (PM) cortex and performing spike-triggered stimulation in the primary sensory cortex (S1).

II. Microdevice System Design & Implementation

A. Microdevice System Architecture

Figure 2 depicts the system architecture of the proposed NHP microdevice. The system is partitioned into two

functional units, namely, a backpack unit (BPU) and a head-mounted unit (HMU). The BPU houses a BLE module (SAMB11, *Atmel*) and power-management circuitry, while the HMU houses an ADS ASIC, a microcontroller unit (MCU; STM8L151G6U6, *STMicroelectronics*), and associated peripheral components. A user base station hosts custom software for bidirectional wireless communication with the HMU via the BLE link as well as a 433-MHz RF receiver for wirelessly capturing the recorded neural data. The architecture of the firmware and software implemented on the user base station and HMU has been detailed previously [4].

The BPU contains a SAMB11 BLE module that relays wirelessly received commands from the user base station to the HMU. Specifically, a universal asynchronous receiver-transmitter (UART) bus is employed to transmit (TX) and receive (RX) data between the SAMB11 BLE module and the MCU following bidirectional level shifting between 3.6V and 1.8V. A buck converter establishes a 1.8-V (V_{MCU}) supply from the battery voltage to provide power to the MCU and two low-dropout (LDO) regulators in the HMU. In turn, these LDOs generate the 1.5-V analog and digital supplies necessary for the ADS ASIC. The main power source of the BPU is a 3.6-V, 1.6-Ah, lithium-ion battery (LTC16M-S4, *Eagle-Picher*), which is connected to the BPU in a plug-and-play fashion for rapid replacement. The power supply level is monitored by measuring the midpoint voltage (V_{MID}) formed between two 1-MΩ resistors connected to the input of the analog-to-digital converter in the SAMB11 BLE module. A screw-down terminal header provides access to V_{MCU}, TX, RX, and ground signals needed to operate the HMU.

The electronic components of the BPU are packaged onto a 4-layer, rigid, printed-circuit board (PCB) measuring 5.4cm × 2.9cm, as shown in Fig. 2. The PCB is coated with a thin, acrylic, conformal coating (419D, *MG Chemicals*) to protect the sensitive circuitry from moisture buildup that could otherwise result from elevated humidity and temperature levels during *in vivo* experimentation. The fully assembled PCB is placed inside an off-the-shelf plastic enclosure box (1551H, *Hammond Manufacturing*) measuring 5.9cm × 3.4cm × 2.0cm. The enclosed BPU is slipped into a lightweight primate jacket for facilitating battery replacement and diagnostic probing. In total, the BPU weighs 35.5g, with the battery and the PCB accounting for 44% and 25%, respectively, of the weight.

The main components of the HMU are the low-power MCU and the ADS ASIC. A shielded, 4-conductor, PVC-jacketed cable (NMUF4/36-2550SJ, *Cooner Wire*) is subcutaneously tunneled from the BPU's terminal header to provide power, serial communication, and ground signals to the HMU. The cable bundle is outfitted with a low-profile microconnector that terminates into a socket on the bottom side of the HMU PCB (see Fig. 2) for design modularity and ease of removal in case of microdevice failure.

The MCU handles the majority of the tasks that require direct interaction with the ADS ASIC. For example, ASIC-level programming operations and other ADS-related routines are carried out through a serial interface comprised of *Clock*, *Data*, *Strobe*, *Trigger*, and *Check* signals.

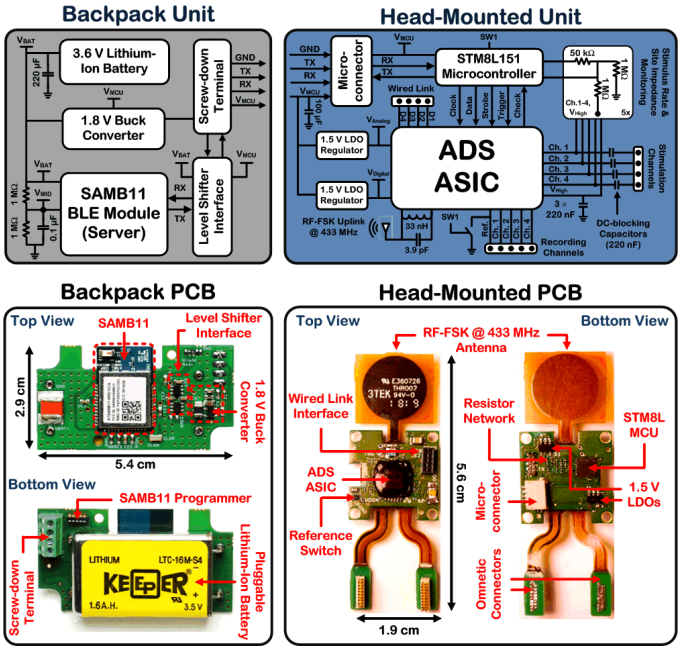

Fig. 2. **Top –** Functional block diagrams of the backpack and head-mounted units. **Bottom –** Photographs of the fully assembled printed-circuit boards for the backpack and head-mounted units.

Peripheral operations such as stimulus rate and site impedance monitoring are performed through a resistive network, which is repeated for each of the four stimulation channels of the ASIC and its "high" voltage output of 5V. If an operation requires aggregation of specific measurements or ASIC status notifications, the MCU sends the appropriate information to the SAMB11 BLE module via the UART interface, where it is subsequently relayed to the user base station via the BLE link.

At the core of the HMU lies the ADS ASIC [5]. A switch controlled by the MCU can change the recording front-end's reference between the system ground and an active site on the recording microelectrode for enhanced ability in common-mode noise rejection. Four-channel neural recordings can be observed temporarily with a custom LabVIEW program via a wired link interface to the ASIC. Single-channel recordings can be captured via the RF-FSK link of the ASIC at 433MHz.

The electronic components of the HMU are packaged onto a 4-layer rigid-flex PCB, with the ASIC wirebonded into place and protected with a high-temperature epoxy encapsulant. The fully assembled PCB in Fig. 2 measures 5.6cm × 1.9cm, including the flexible extrusions at each end. At the top end of the PCB, a square-shaped polyimide arm (1.7cm × 1.5cm) encloses a flexible antenna for the 433-MHz RF-FSK transmitter. At the bottom end, two flexible polyimide arms terminate into two rigid islands, each housing an Omnetics microconnector (A79039-001, *Omnetics*). These microconnectors interface directly with two single-shank, 16-channel, Michigan-style, recording and stimulating microelectrodes (H-16, *NeuroNexus Technologies*) implanted in the PM and S1 cortical areas, respectively.

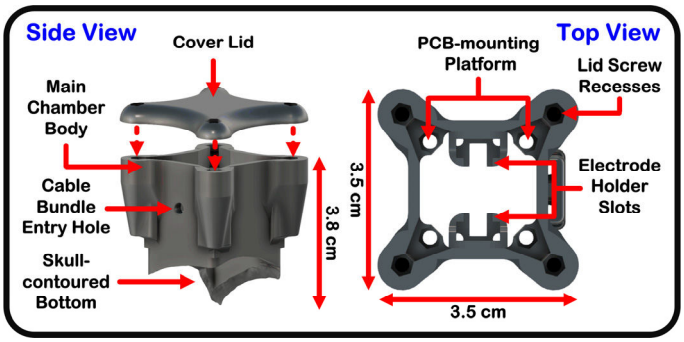

Fig. 3. A render of the skull-affixed, 3D-printed, resin, primate chamber. Hex-shaped recesses allow for the printed-circuit board and the lid to be screwed into place.

To protect the sensitive circuitry of the HMU from potential moisture buildup and limit liquid and vapor water ingress due to elevated humidity and temperature levels encountered during *in vivo* experimentation, the HMU PCB is encapsulated by a 5-µm layer of Parylene–C applied via chemical vapor deposition (CVD; *SMART Microsystems*). Prior to deposition, the board is cleaned in a 50°C ultrasonic bath consisting of 10% flux solvent (*MG Chemicals*) and 90% de-ionized water by volume to ensure the removal of contaminants that may interfere with layer adhesion or facilitate corrosion due to metal-ion reactions. In total, the HMU weighs 12.5g, with the chamber accounting for 87% of the weight.

B. Design of HMU Chamber and System Assembly

Figure 3 depicts a render of the custom 3D-printed resin chamber measuring 3.5cm × 3.5cm × 3.8cm. This chamber protects the HMU PCB and creates a sterile barrier between the external environment and the exposed implant area. To minimize pathways for infection around the implant site, the chamber's bottom side is contoured to follow the topography of an adult squirrel monkey's skull. Directly above the skull-contoured region, two slots protrude from the chamber's inner walls to hold the electrode microconnectors in place, and four standoff hex-shaped recesses create a mounting platform for the HMU PCB. A small opening slightly beneath the platform allows the subcutaneously tunneled cable bundle to enter the chamber and terminate into the HMU PCB. Finally, a lid is attached to the chamber with a set of screws. A silicone sheet is added between the chamber and the lid to act as a watertight gasket for completely sealing the chamber once closed.

Before affixing the chamber to the primate's skull, the entire system is assembled into a single monolithic unit as shown in Fig. 4. First, the microelectrode shanks are lowered into their respective slot holders. Next, a portion of the cable bundle is threaded through the chamber's entry hole and connected to the HMU PCB, which is then lowered into the chamber with the flexible arms bent underneath the board to interface with the electrodes' microconnectors. Once the microconnectors are seated, the HMU PCB is fixed onto the standoff platform with screws. The flexible antenna is then bent over the board, and the lid is screwed into place.

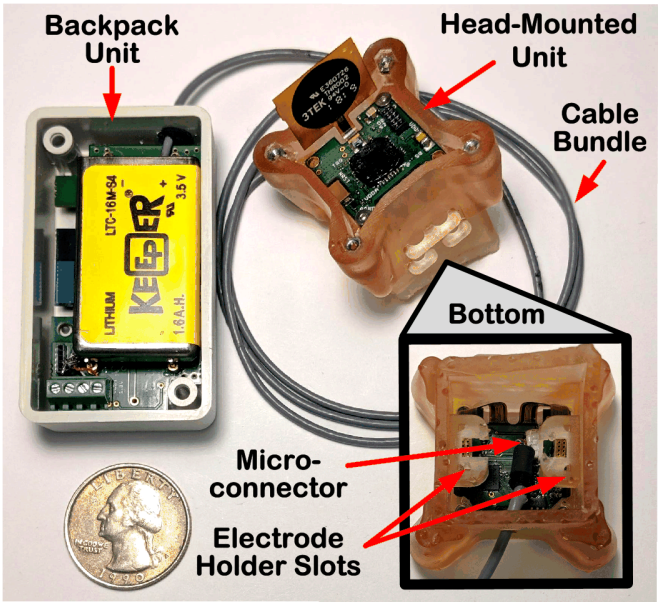

Fig. 4. Photographs of the fully assembled backpack and head-mounted units connected by a subcutaneously tunneled cable bundle. Lids accompany both units when deployed.

The final unit is sterilized with ethylene oxide (EtO) gas and attached to the skull with dental acrylic. Finally, the cable bundle is guided subcutaneously from the HMU toward the BPU located in a primate jacket. The entire NHP microdevice weighs ~48g.

III. Measurement Results

To verify the overall functionality of the microdevice, *in vitro* experiments were conducted with the system configured as depicted in Fig. 4. Acute microelectrode arrays were attached to the HMU PCB and submerged in saline. In each experiment, digitized neural activity prerecorded from the PM region of freely moving rodents was played into the saline solution, with a silver-chloride wire as the return electrode.

In the first phase of experimentation, raw 4-channel recordings were analyzed in LabVIEW via the wired link interface of the ASIC. Figure 5 (top) depicts a 1.8-sec window of the raw recordings obtained from one channel of the ASIC. These recordings were then processed offline with a custom script to obtain the parameters for spike discrimination based on thresholding and time-amplitude windowing. These parameters were wirelessly programmed into the ASIC from the user base station via the BLE link, and the recording process was repeated. Figure 5 (bottom) depicts a graph of superimposed time-aligned neural signals discriminated during the recording. It can be observed that the accepted waveforms, indicated with red stars (top) and black traces (bottom), satisfied all the criteria for thresholding/time-amplitude window discrimination, while other waveforms, shown in light gray (bottom), did not and were thus rejected.

In the second phase of experimentation, the ASIC's stimulating back-end and RF-FSK wireless link were verified.

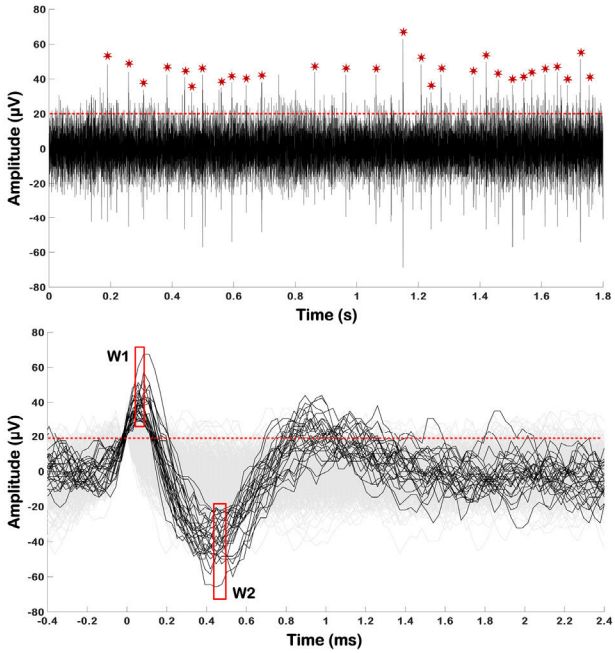

Fig. 5. **Top** – A 1.8-sec window of neural activity recorded *in vitro* from saline. Red stars indicate the neural spike waveforms accepted by the ASIC's spike discriminator for stimulus triggering. **Bottom** – Superimposed and time-aligned neural spike waveforms from the above recording. Spike waveforms that cross the activation threshold of 20μV (red-dashed line) and subsequently pass through both time-amplitude windows (red rectangles) are plotted in black. Rejected waveforms are plotted in light gray.

The ASIC was programmed with the spike discrimination parameters obtained in the first phase in order to trigger stimulation in response to the discriminated neural spikes. For each trigger event, a single monophasic current pulse (40μA, 192μs) with passive discharge was delivered through the stimulating electrode to the saline. This was followed by a 3.5-ms blanking period in order to reject any transient stimulus artifacts that could be mistaken for neural activity. Figure 6 shows graphs of superimposed discriminated neural spike waveforms obtained wirelessly via the RF-FSK link. Also shown are the corresponding stimulus artifacts from the appropriately triggered stimulus pulses, with spike-stimulus delays of 2ms and 4ms. This demonstrates the correct functionality of the NHP microdevice for ADS.

Finally, the effectiveness of the Parylene–C encapsulant was verified *in vitro* on partially populated test boards, which were absent of the ASIC and the two Omnetics microconnectors. Levels of moisture ingress were observed by monitoring microdevice current consumption, as well as by shorting the primary stimulation sites to the 1.8-V supply rail to monitor internal resistance changes through the microdevice's site impedance monitoring function. Two microdevices were prepared, cleaned, and coated before being placed into a covered glass container lined with damp towels. This test chamber was then placed on a hotplate to generate an elevated temperature and humidity environment. Each board was rested upon one of the aforementioned resin chambers to prevent direct contact with the heat and moisture sources, while still allowing ample vapor circulation to both sides of the board.

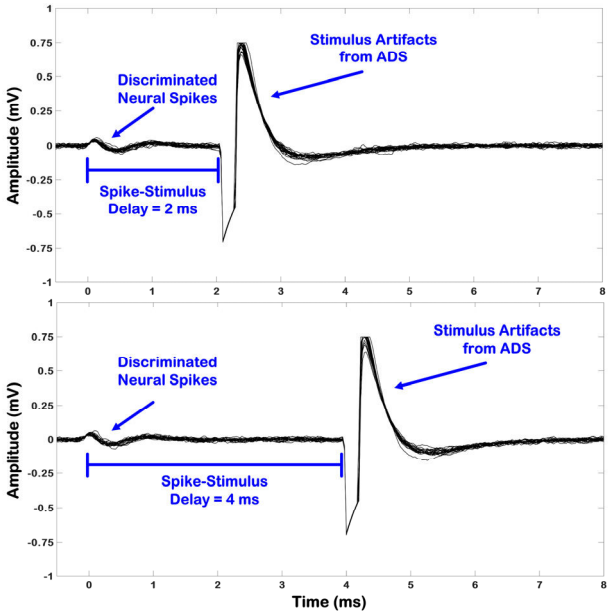

Fig. 6. Graphs of superimposed neural spike waveforms discriminated by the ASIC along with corresponding stimulus artifacts resulting from ADS with spike-stimulus delays of 2ms and 4ms. The waveforms are recorded wirelessly, with the amplitudes referred to the input.

Over a 2-week monitoring period, the current consumption of both microdevices showed an average fluctuation of less than ±5%, with no observed deviation of stimulation site voltages from their 1.8-V baseline value.

IV. Conclusion

This paper reported on the design and development of a BLE-enabled microdevice for ADS applications in nonhuman primates. Comprising miniaturized head-mounted and backpack units outfitted in compact enclosures, the overall microdevice is lightweight (~48g), mechanically stable, and resistant to elevated levels of temperature and humidity for 2 weeks when encapsulated by a 5-μm layer of Parylene–C. Furthermore, *in vitro* testing in saline established the microdevice's ability to record and discriminate neural spike waveforms, and subsequently perform appropriately timed spike-triggered stimulation.

References

[1] D. J. Guggenmos, et al., "Restoration of function after brain damage using a neural prosthesis," *Proc. Natl. Acad. Sci. USA (PNAS)*, vol. 110, no. 52, pp. 21177-21182, Dec. 2013.

[2] J. G. McPherson, et al., "Targeted, activity-dependent spinal stimulation produces long-lasting motor recovery in chronic cervical spinal cord injury," *Proc. Natl. Acad. Sci. USA (PNAS)*, vol. 112, no. 39, pp. 12193-12198, 2015.

[3] M. Azin, et al., "A miniaturized system for spike-triggered intracortical microstimulation in an ambulatory rat," *IEEE Trans. Biomed. Eng.*, vol. 58, no. 9, pp. 2589-2597, Sep. 2011.

[4] N. H. Vitale, M. Azin, and P. Mohseni, "A Bluetooth Low Energy (BLE)-enabled wireless link for bidirectional communications with a neural microsystem," in *Proc. IEEE Biomed. Circ. Syst. Conf. (BioCAS)*, pp. 371-374, Cleveland, OH, Oct. 2018.

[5] M. Azin, et al., "A battery-powered activity-dependent intracortical microstimulation IC for brain-machine-brain interface," *IEEE J. Solid-State Circuits*, vol. 46, no. 4, pp. 731-745, Apr. 2011.